Available online at www.sciencedirect.com
ScienceDirect
Journal of Molecular Catalysis A: Chemical 265 (2007) 141–147
JOURNAL OF MOLECULAR CATALYSIS A: CHEMICAL
www.elsevier.com/locate/molcata

Model Pd-based bimetallic supported catalysts for nitrate electroreduction

S.N. Pronkin [a,b,*], P.A. Simonov [a], V.I. Zaikovskii [a], E.R. Savinova [a]

[a] *Boreskov Institute of Catalysis, SB RAS, 630090 Novosibirsk, Russia*
[b] *Moscow State University, Faculty of Chemistry, Department of Electrochemistry, 119998 Moscow, Russia*

Received 19 July 2006; received in revised form 5 October 2006; accepted 5 October 2006
Available online 12 October 2006

Abstract

An approach for *in situ* preparation of bimetallic Pd–Cu catalysts active in nitrate electroreduction is described. The catalysts are prepared by modification of the surface of Pd carbon-supported nanoparticles by monolayer of Cu. The morphology of Pd/C nanoparticles is characterized by HR-TEM and by their electrochemical properties in the adsorption of hydrogen and Cu adatoms. Modification of Pd surface by Cu adlayer results in significant increase of the activity in nitrate electroreduction. Dependencies of the reaction rate for Cu/Pd/C catalysts on the electrode potential, nitrate concentration and anion of supporting electrolyte are discussed.

Keywords: Nitrate reduction; Palladium; Nanoparticles; Electroreduction; Cu upd; Bimetallic catalysis

1. Introduction

Since the pioneering work of Tacke and Vorlop [1,2] liquid phase catalytic reduction has been recognized as a promising method for purification of industrial and domestic water supplies from nitrate/nitrite contaminations. Contrary to other techniques, as reverse osmosis, dialysis or ion-exchange, catalytic reduction offers the means of selective conversion of hazardous nitrate/nitrite toward harmless nitrogen. Investigations of the nitrate reduction by reducing agents (hydrogen, formic acid) on the surface of metal catalysts in aqueous solutions [2–5] have resulted in the general reaction scheme represented in Fig. 1. It is believed that the role of reductants is to impart negative charge on metal catalysts. The latter adsorb hydrogen through the discharge of solvent molecules and act as microelectrodes reducing nitrate ions. On many metals (including Pt, Pd, Cu and Rh) the rate determining step (rds) is supposed to be the reduction of the adsorbed nitrate into nitrite, II [3,5]. Further reduction of nitrite can yield several possible products: nitrogen, which may be formed directly from intermediate NO_{ads} or *via* formation of N_2O, ammonia and hydroxylamine [2,4]. For water purification the target product is N_2, since the other products are relatively toxic. For example, the maximal permitted concentration of ammonia in drinking water according to EU regulations is 50 times lower than that of nitrate.

Pd shows outstanding selectivity in nitrite and NO reduction to N_2. However, its activity in step (II) is low and promoting additives are required to accelerate the overall process. Bimetallic Pd-based catalysts (Pd–Cu [1,2,4–9], Pd–Sn [2,4,8,10], Pd–In [2,4]) have been recognized as having the highest activity and selectivity in nitrate reduction to N_2. Despite several attempts, the structure and composition of catalysts for the nitrate reduction has not yet been optimized due to a number of reasons, among which:

- The reaction rate and selectivity result from a complex interplay of the structure of the active component, the support nature [7,10], and the reaction conditions: pH, concentrations, etc. [2,10].
- Little is known about the catalyst structure *in situ*, even less (if any) about its surface composition.
- The role of promoters in nitrate reduction has not yet been established. Some authors proposed formation of mixed bimetallic active sites [4], while the other assumed parallel redox reactions on electrically connected Pd and promoter sites ("local cell" mechanism), [11] or even independent processes on the two components [7].

* Corresponding author at: Boreskov Institute of Catalysis, SB RAS, 630090 Novosibirsk, Russia. Tel.: +7 3833 30 75 63; fax: +7 3833 30 80 56.
E-mail address: sprn@catalysis.ru (S.N. Pronkin).

1381-1169/$ – see front matter © 2006 Elsevier B.V. All rights reserved.
doi:10.1016/j.molcata.2006.10.007

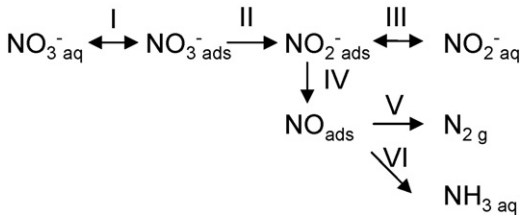

Fig. 1. General scheme of liquid-phase catalytic reduction of nitrate [2,4,5].

Electrocatalytic reduction of nitrate on Pd and Pd-M electrodes, on the one hand, may significantly advance understanding of the catalytic reaction mechanism [11,12], and on the other hand offers a promising approach towards water purification. If indeed the role of a reductant is restricted to charging the metal surface, so that it does not directly interact with nitrate as claimed e.g. in Ref. [13], heterogeneous catalytic and electrocatalytic processes are likely to follow similar reaction schemes. Electrochemical approach offers several advantages in comparison to the conventional liquid phase catalysis.

- The interfacial potential drop at the metal|liquid interface can be finely tuned and controlled by the electrode potential, and the reaction rate is proportional to the current and easy to measure.
- Electrons act as a convenient and easy-to-handle reductant producing adsorbed hydrogen on the catalyst surface by the discharge of water (protons).
- Bimetallic surfaces can be created *in situ* under reaction conditions by (a) adsorption of metal adatoms [3,14–17], (b) co-electrodeposition [18] or (c) electroreduction of spontaneously adsorbed precursors [19].
- The surface composition of bimetallic electrodes can be characterized *in situ* by their electrochemical response which gives an unprecedented opportunity to link the catalyst structure, composition with its catalytic activity.

Electroreduction of nitrate has been studied on various metal electrodes including Pt [13–15], Rh [20], Pd [14] and Cu [21]. Comparative study on various transition and coinage metals was performed by Koper et al. [12]. The results of electrocatalytic studies of nitrate reduction on Pd and Pd-M, combined with DEMS analysis of reduction products, allowed to clarify some details of the reaction mechanism and provided a better understanding of the function of bulk bimetallic catalysts [3,12]. It was demonstrated that selectivity toward N_2 formation increases with Pd content and is governed by the ratio of surface coverages of nitrogen-containing (formed preferentially on Cu sites) and hydrogen-containing (formed on Pd sites) adsorbates. Nitrite formed in step II is reduced rapidly to NO_{ads}, the latter on pure Pd being selectively reduced to N_2. On contrary, NO and N_2O desorb from bulk Cu as the reaction products [12].

So far, studies of electrocatalytic reduction of nitrate have been restricted to bulk polycrystalline electrodes. This work is to our knowledge the first attempt to perform electrocatalytic nitrate reduction on supported bimetallic nanoparticles. The goal was to establish a method for the preparation of well defined Pd–Cu nanoparticle catalysts and to explore their interfacial and electrocatalytic properties in nitrate reduction.

2. Experimental details

2.1. Catalyst preparation and characterization

Pd/C catalysts were synthesized by the deposition method [22]. Low surface area ($\sim 6\,m^2\,g^{-1}$ BET specific surface area) non-activated carbon of the Sibunit family (see Ref. [23] for the preparation and properties of carbon materials of the Sibunit family), was used as a catalyst support in order to avoid problems associated with the mass transport in the pores. The support was impregnated with a concentrated H_2PdCl_4 solution and after dilution with water the resulting mixture was vigorously stirred for 20 min in air. Pd hydroxide was then deposited on carbon by the drop-wise addition of Na_2CO_3 solution upon continuous stirring. The slurry was aged for 30 min at room temperature, washed with water until neutral and dried at 110 °C. Finally the catalyst was reduced with H_2 in a flow reactor at 100 °C for 20 min and then at 150 °C for another 20 min.

The size of Pd particles was adjusted by varying the concentration and the amount of H_2PdCl_4 and Na_2CO_3 solutions. For the present study, two Pd/C samples were prepared with 5 wt.% Pd (S1) and 3 wt.% Pd (S2). The size and structure of carbon-supported Pd particles were characterized by high resolution electron microscopy (HR-TEM) with microscope *JEM-2010* (JEOL, Japan) with a lattice-fringe resolution of 0.14 nm at an accelerating voltage of 200 kV. Samples to be examined by HRTEM were prepared on a perforated carbon film mounted on a copper grid.

2.2. Electrochemical measurements

Electrochemical measurements were carried out with *Autolab PGSTAT 30* potentiostat in a three-compartment electrochemical cell comprising a working electrode, a counter electrode (Pt foil) compartment separated by a glass frit and a reference electrode (mercury sulfate or trapped hydrogen electrode) compartment connected *via* Luggin capillary. Potentials are quoted against reversible hydrogen electrode in the same solution. Solutions were purged with high purity Ar (99.998%) before measurements. All experiments were performed in thermostatic conditions at 25 ± 0.1 °C.

Electrochemical properties of powder catalysts were studied using a slightly modified thin layer method introduced by Schmidt et al. [24]. A glassy carbon (GC) cylinder was used as a substrate for the working electrode preparation. The cylinder was placed into a Teflon holder (with a brass current collector) and sealed with the Teflon tape so that only the flat bottom part of the cylinder ($S = 0.20\,cm^2$) was exposed to electrolyte. The absence of a leakage through the sealing was checked by measuring capacitive currents in supporting electrolytes. After electrochemical characterization of bare GC electrode it was rinsed with water and dried under the stream of Ar. About

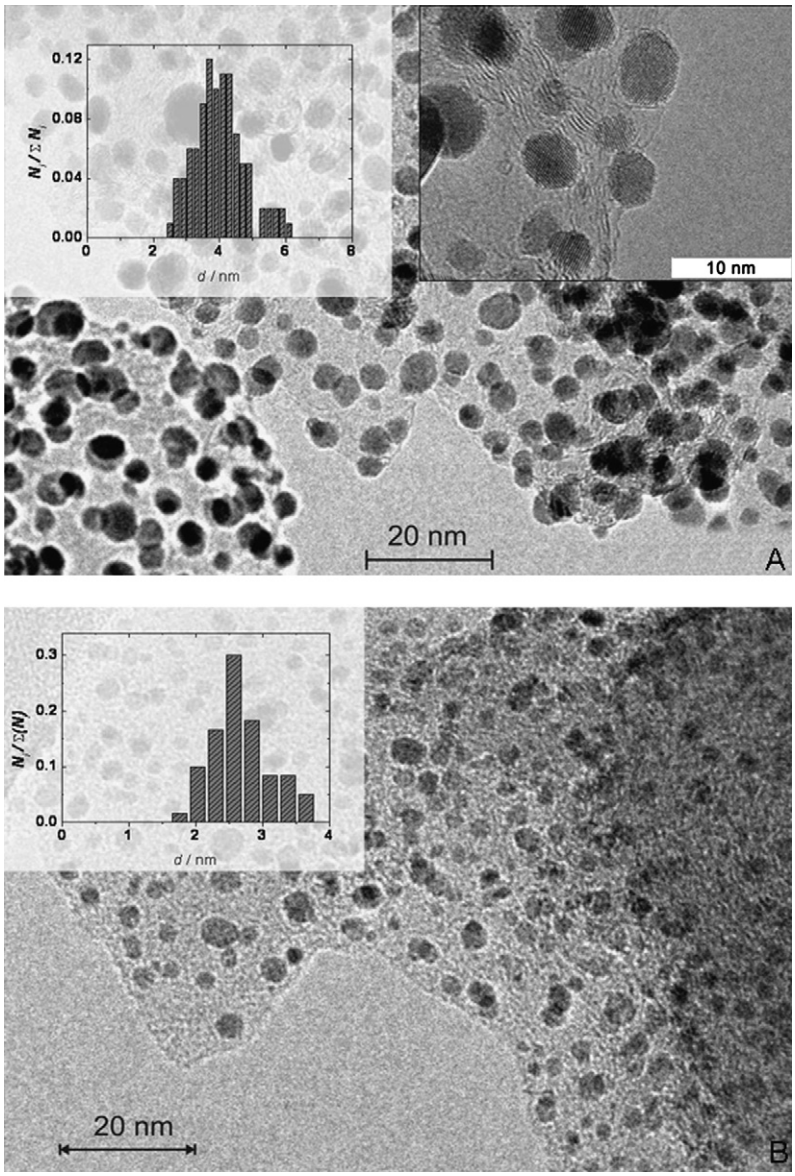

Fig. 2. HRTEM images and typical size distributions for Pd/C samples S1 (A) and S2 (B).

20 μl of freshly agitated catalyst suspension (3 mg ml^{-1} (S1) or 2.5 mg ml^{-1} (S2) in water sonicated for 40 min) were pipetted on the flat part of GC cylinder and dried under Ar at room temperature for 60 min. After this the electrode was again rinsed thoroughly with water and immersed in the electrochemical cell at controlled potential in the double layer region of Pd. This procedure ensured high reproducibility and stability of the catalyst layer without the addition of Nafion® ionomer. The resulting catalyst loading was 7.5–15 μg cm^{-2} (per GC geometric area).

2.3. Glassware and solutions

Solutions were prepared with MilliQ water (18 MΩ cm^{-1}). Suprapure concentrated acids were used for the preparation of H_2SO_4 and $HClO_4$ supporting electrolytes. Analytical grade salts were recrystallized from water twice and then used for the preparation of $CuSO_4$ and $NaNO_3$ solutions.

The glassware was cleaned by soaking in fresh H_2SO_4:H_2O_2 (1:1 vol) mixture and thoroughly washing with MilliQ water before the experiments.

3. Results and discussions

3.1. Electron microscopy

TEM images of Pd/C(S1) and Pd/C(S2) samples are represented in Fig. 2A and B correspondingly. Particle size distributions were constructed for at least 100 particles in each image. The distributions for different parts of large-scale images were well reproducible. The mean particle size $d = \sum_i n_i d_i / \sum_i n_i$ calculated from the size distributions was 4.0 and 2.6 nm for Pd/C(S1) and Pd/C(S2), respectively.

For particles with $d \geq 2$ nm the metal lattice is clearly resolved at high magnifications (inset of Fig. 2A). Particles larger than 4 nm are facetted, while the smaller ones have spherical shapes.

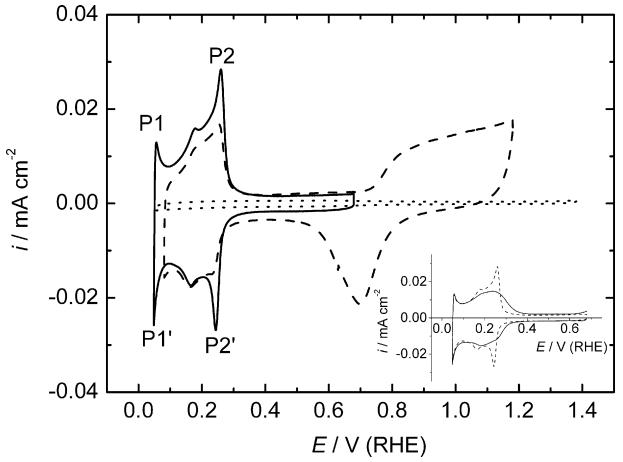

Fig. 3. CVs for Pd/C(S1) in 0.1 M H_2SO_4 at 10 mV s^{-1} obtained for different upper potential limits. CV for bare GC electrode is shown as a dotted line for comparison. In the inset CVs for Pd/C(S1) in 0.1 M H_2SO_4 (dashed) and 0.1 M $HClO_4$ (solid) are compared.

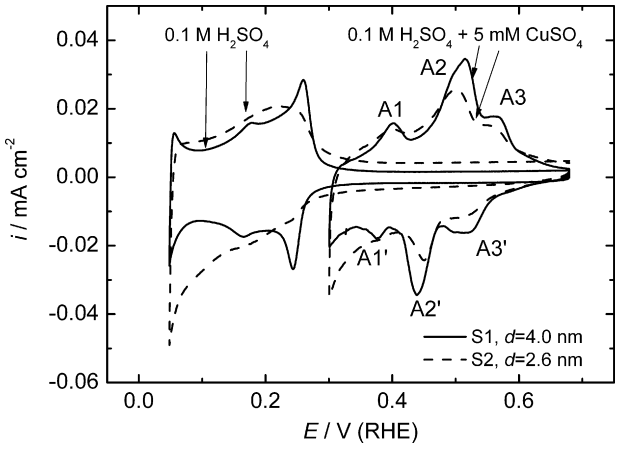

Fig. 4. CVs for Pd/C electrodes in 0.1 M H_2SO_4 (S1 solid, S2 dashed) and 0.1 M H_2SO_4 + 5 mM $CuSO_4$ (S1 solid, S2 dashed), 10 mV s^{-1}.

3.2. Electrochemical properties of Pd/C samples

A typical cyclic voltammetry (CV) curve for Pd/C(S1) electrode in 0.1 M H_2SO_4 is represented in Fig. 3. The solid trace corresponds to the steady-state response, which is recorded after the first potential excursion down to 0.05 V. During the first scan (not shown) the charge transferred in the cathodic sweep exceeds that of the anodic indicating reduction of Pd oxide formed on the surface of nanoparticles in contact with the ambient atmosphere. The increase of the current below 0.06 V (P1/P1′) is attributed to the absorption of hydrogen in the Pd bulk [25,26]. Above 0.06 V three potential ranges typical of Pt group metals are distinguished: the "hydrogen" range ($E < 0.32$ V) where adsorbed hydrogen is formed on the surface, the double-layer range ($0.32 < E < 0.70$ V on the positive-going sweep) and the "oxygen" range (above 0.70 V) where oxygen-containg adsorbates are formed through water dissociative adsorption.

In the inset of Fig. 3 CVs in 0.1 M H_2SO_4 and 0.1 M $HClO_4$ are compared. The absence of peaks P2/P2′ in $HClO_4$ indicates that sulfate adsorption/desorption is involved in the process responsible for these peaks in H_2SO_4. This has been confirmed in studies on vicinal Pd single crystal electrodes [27–29] which have clearly demonstrated that peaks P2/P2′ are related to sulfate adsorption on ordered (1 1 1) and (1 0 0) surface domains. No such peaks were detected for Pd(1 1 0) electrodes. Comparing the sharpness of the peaks for Pd/C nanoparticles with those observed for high index Pd(*h k l*) surfaces with various (1 1 1) terrace width, one may roughly estimate the average size of ordered domains on nanoparticles as ~1.5 nm. Similarly to what has previously been observed for single crystals [30], an excursion to the "oxygen" potential range results in a significant depression of P2/P2′ peaks and in the irreversible change of the CV response due to Pd anodic dissolution (dashed curve in Fig. 3). Meanwhile, when the upper potential limit does not exceed 0.7 V, the voltammetric response does not change within several hours of measurements confirming the stability of Pd/C(S1).

Fig. 4 compares the CVs for Pd/C samples with two different average particle sizes. For smaller particles of Pd/C(S2) P2/P2′ the CV peaks are much weaker or even absent, being in agreement with HRTEM data which give evidence of the absence of facets on smaller particles. The origin of higher cathodic currents at $E < 0.15$ V for small particles compared to large ones is not fully understood yet. It cannot be attributed to the hydrogen absorption, since an anodic counterpart is absent on the reverse potential sweep. We tentatively attribute the cathodic current increase at $E < 0.15$ V either to the onset of the hydrogen evolution reaction (due to the positive size effect) or to the reduction of surface oxide by adsorbed hydrogen.

In contrast with Pd/C(S1), the CVs for Pd/C(S2) are unstable demonstrating continious current decrease (ca. 8–12% during 600–700 s of potential cycling) even if the upper potential limit does not exceed 0.7 V. We tentatively impute this to slow Pd dissolution. Due to higher stability of S1 sample, we perfomed most of electrochemical and electrocatalytic measurements with larger particles, while for selected conditions the properties of these electrodes were compared with S2 to detect possible structural effects.

Underpotential (upd) metal deposition (i.e. deposition of metal adatoms on foreign metal surfaces above their reversible potential) is known to be very sensitive to the surface structure and crystallography. In this work adsorption of Cu adatoms was used to obtain *in situ* information on the structure of Pd nanoparticles. In Fig. 4 CV responses of Pd/C electrodes in 0.1 M H_2SO_4 and 0.1 M H_2SO_4 + 5 mM $CuSO_4$ are represented. The deposition of bulk metallic Cu occurs below 0.29 V (which corresponds to Cu^{2+}/Cu^0 reversible potential estimated neglecting activity coefficients). The Cu upd region where adsorbed monolayer of Cu on Pd surface is stable due to Cu–Pd interaction extends ca. 0.35 V positive of the reversible Cu^{2+}/Cu^0 potential. Three pairs of anodic/cathodic peaks of Cu upd are observed on Pd/C samples in agreement with the literature data for electrodeposited Pd [16,17]. Comparison of the CVs for electrodeposited Pd possessing no preferential orientation with ones for basal Pd single crystals allows tentative assignment of these peaks [31]. A1/A1′ and A3/A3′ may be assigned to Cu upd on Pd(1 0 0) and A2/A2′—on Pd(1 1 1). LEED study of Cu upd on Pd(1 0 0) demonstrated that peaks A3/A3′ are due to

formation/dissolution of ordered $c(2 \times 2)$ Cu adlayer [32], while to the best of our knowledge no information on the structure of ordered Cu adlayers on Pd(1 1 1) has been published.

The CV peaks of Cu upd observed in the present work for Pd nanoparticles are much broader and less intense than those measured on single crystal Pd electrodes and decrease with the decrease of the particle size (*cf.* CVs for Pd/C(S1) and Pd/C(S2) in Fig. 4). From this we conclude that Pd(1 1 1) and Pd(1 0 0) facets are present on Pd/C(S1) nanoparticles, but their dimensions decrease with the decreasing particle size. Measurements of the charge of Cu upd is one of the most suitable ways of *in situ* determination of Pd surface area [16,33]. The charge passing during Cu monolayer deposition (Q_{Cu}) was estimated as 0.42 mC cm^{-2} for Pd with no preferential surface orientation and as 0.48 mC cm^{-2} for Pd(1 1 1) [34], the difference being attributed to the contribution of sulfate adsorption. Considering small dimensions of the ordered crystalline domains on Pd nanoparticles, we used the value of the monolayer charge of Cu for polycrystalline Pd when estimating their surface area. The ratio of Cu adsorption (Q_{Cu}) and hydrogen sorption (Q_{HA}) charges for samples S1 and S2 was calculated to be 1.90 ± 0.03 and 2.00 ± 0.05, respectively. This ratio is considerably higher than that observed for Pd electrolytic deposits (0.06–0.17 depending on the conditions of Pd deposition [16]). Since the adsorption of hydrogen monolayer on polycrystalline Pd surface requires 0.21 mC cm^{-2}, the value $Q_{Cu}/Q_{HA} \approx 2$ indicates that hydrogen *absorption* is negligible for Pd nanoparticles in the potential interval explored. The hydrogen absorption capacity of nanoparticles with $d_m \approx 4$ nm has been estimated as being only ca. 15% smaller than that for bulk Pd in Ref. [35]. The combined electrochemical and *in situ* EXAFS study of Rose et al. [26] supports a H/Pd ratio of 1 at potentials between 0.05 and 0.028 V for 40% Pd/C catalyst from E-Tek. Thus, negligible contribution of hydrogen absorption for Pd/C samples observed in this work in the potential interval explored can be attributed to the negative shift of the onset of this process due to the particle size effect. Suppression of hydrogen absorption has been previously observed for Pd nanoparticles supported on glassy carbon by vapor deposition [36] and mixed Pd–Pt nanoparticles prepared by water-in-oil microemulsion technique [37].

3.3. Preparation of bimetallic Pd–Cu surface

Podlovchenko et al. [16,17,25] developed a convenient tool for an *in situ* preparation of Pd–Cu bimetallic surfaces by Cu upd on electrodeposited Pd. De Vooys et al. [3] have used this approach to prepare active Pd–Cu catalysts for nitrate electroreduction. Since the amount of Pd in electrodes utilized in this work was very small (1.5–3 μg), even a short contact with the ambient atmosphere upon transfer from the Cu deposition into the reaction cell resulted in irreversible loss of Cu adlayer. Thus, a different approach has been developed in this work for formation of Cu adlayers with controllable surface coverage on Pd nanoparticles.

First, Pd nanoparticles were covered with excessive amounts of Cu (more than three monolayers was necessary to ensure conservation of Cu deposit during the transfer). The samples produced are addressed as Cu/Cu/Pd/C. Then, the electrode was transferred into the reaction cell filled with supporting electrolyte. In order to remove multilayer Cu from the particle surfaces, the electrodes were subjected to 0.35 V for 120 s under vigorous solution agitation. The current during the dissolution was monitored in order to ensure multilayer Cu removal. Thus prepared samples with (sub)monolayer Cu coverage were designated as Cu/Pd/C. Concentration of Cu ions in the reaction cell resulting from partial dissolution of Cu was estimated as $<10^{-7}$ M and was neglected in the further analysis. The absence of Cu deposition from the supporting electrolyte during the activity measurements is supported by the experimental results as further discussed in the text.

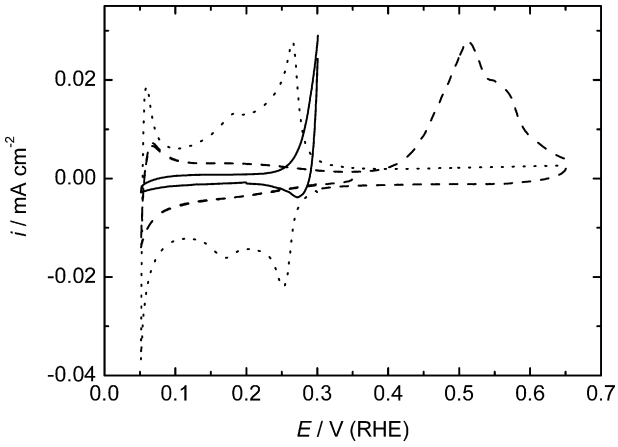

Fig. 5. CV responses of Cu-modified Pd/C (S1) electrode in 0.1 M H_2SO_4, 10 mV s^{-1}. Solid: CV after the transfer (Cu/Cu/Pd/C); dashed: after multilayer Cu oxidation (Cu/Pd/C); dotted: after complete Cu dissolution (bare Pd/C), see text for details.

CV response of Cu/Cu/Pd/C(S1) is shown as the solid trace on Fig. 5. The currents of hydrogen adsorption/absorption on Pd are completely suppressed. The currents in the range above 0.25 V can be attributed to the dissolution of the multilayer Cu. The CV of Cu/Pd/C(S1) electrode obtained after the dissolution of Cu exceeding one monolayer is shown as a dashed trace in Fig. 5. If the upper potential limit is kept below 0.35 V, this curve is steady-state, indicating stability of the surface towards Cu dissolution in the electrolyte or in the Pd particle bulk, at least on the time scale of the measurements (few hours). A potential scan to the higher values results in the oxidation of Cu adlayer and in the irreversible change of CV curve, which becomes identical to the CV of the bare Pd surface (dotted trace). We conclude that by dissolution of multilayer Cu at 0.35 V, a Cu adlayer is formed on the surface of Pd nanoparticles, which can be removed only at potentials above ca. 0.4 V. From the charge passing during the dissolution of (sub)monolayer Cu, we estimated the Cu coverage as $\theta_{Cu} \approx 0.85$. Smaller Cu coverages can be obtained by partial oxidation of the Cu adlayer, e.g. by controlling the upper limit of the potential scan. Thus, by the suggested technique we are able to create *in situ* bimetallic Pd–Cu catalysts with well defined structure and surface composition which can be varied in a wide range. This approach was successfully applied for studying the dependence of electrocatalytic properties of Cu/Pd/C electrodes

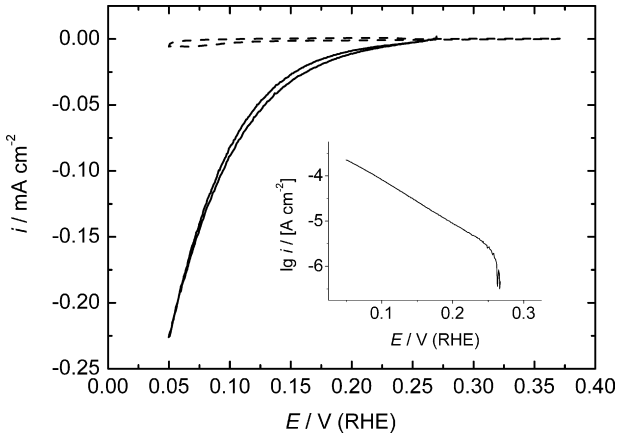

Fig. 6. Stationary polarization curves for nitrate reduction on Pd/C (S1) (dashed) and the same sample covered with 0.85 ML of Cu (solid) in 0.1 M H_2SO_4 + 0.1 M $NaNO_3$ (1 mV s^{-1}). The inset shows Tafel plot of the latter.

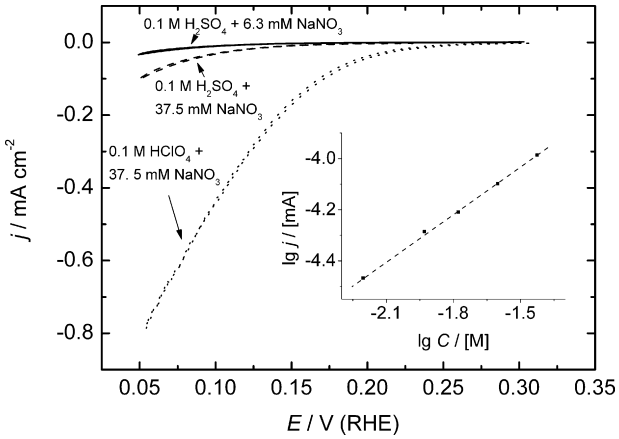

Fig. 7. Nitrate reduction polarization curves for PdCu/C S1 at various concentrations of $NaNO_3$ in $HClO_4$ and H_2SO_4. The inset shows log j vs. log C plot for 0.1 M H_2SO_4 + x mM $NaNO_3$ at E = 0.05 V.

on their surface composition, which will be the topic of the future publication [38].

3.4. Nitrate reduction on Pd–Cu/C

To explore electrocatalytic properties of Cu/Pd/C electrodes, we performed the study of nitrate electroreduction on a bimetallic electrode with $\theta_{Cu} = 0.85$. In order to ensure the stability of Cu adlayer, $NaNO_3$ was added to the cell containing 0.1 M H_2SO_4 at $E = 0.25$ V under continuous Ar purging after the preparation of Cu/Pd/C sample as discussed in Section 3.3. The activity was characterized by linear sweep voltammetry at a slow (1 mV s^{-1}) scan rate (Fig. 6). Stationary character of measured currents was ensured by their independence on the scan rate below 2 mV s^{-1}. The latter fact and the reproducibility of polarization curves in the first and subsequent scans confirm the assumption made in Section 3.3 on the absence of slow Cu redeposition from the solution during the electrocatalytic tests.

The currents were insensitive to the solution stirring indicating kinetic control. Comparison of the nitrate reduction currents on "bare" and Cu-modified Pd/C electrodes (Fig. 6) shows ca. 12 times increase of the catalytic activity in the presence of Cu in 0.1 M H_2SO_4 + 0.1 M $NaNO_3$ solution, thus confirming the promoting effect of Cu in agreement with the previous electrochemical and catalytic studies [3,15]. Comparison of our results with the literature data suggests that the electrocatalytic activity of Cu-modified Pd nanoparticles is comparable with that reported for electrodeposited Pd in Ref. [3]. Tafel plot of the polarization curve shows rather wide linear range with the slope $b = (\partial E/\partial \log i)_C \approx 105$ mV (Fig. 6, inset) at constant nitrate concentration. This value is indicative of one-electron electrochemical rds in agreement with the literature data [12,13]. It corresponds very well to the value reported for Cu adlayers on electrodeposited Pd (110 mV dec^{-1} [3]) and is somewhat lower than the value reported for bulk Cu (130 mV dec^{-1} [12]). From the polarization curves measured at different $C(NO_3^-)$ (Fig. 7) we determine the reaction order versus nitrate at various electrode potentials. It was found that $(\partial \log i/\partial \log C)_E \approx 0.60$ in the potential interval from ~0.05 to 0.12 V and decreases with the electrode potential reaching ca. 0.3 at 0.25 V. Measured reaction order is well below 1, similarly to what has previously been reported for Pd–Cu catalysts [11] and electrocatalysts [3,11] (0.7), as well as for Pt (0.51) and Rh (0.34) electrodes [12], and points out that adsorbed species is involved in the rds. The potential dependence of the reaction order strongly suggests that this intermediate is negatively charged.

To explore the anion effect on the reaction rate of nitrate reduction, currents observed in $HClO_4$ and H_2SO_4 solutions were compared (Fig. 7, dotted and dashed). Remarkably higher currents were detected in $HClO_4$, indicating strong suppression of nitrate reduction by sulfate. This is in agreement with electrochemical studies on Pt, Rh and Pd–Cu electrodes [3,12]. The sensitivity of nitrate reduction to the specific anion adsorption was neglected in some liquid-phase catalytic studies where solution buffering was attained by an addition of HCl. Meanwhile, the specific adsorption of Cl^- anions is known to be remarkably stronger than the one of SO_4^{2-}.

On smaller particles (S2) very similar polarization curves and kinetic parameters (b and $(\partial \log i/\partial \log C)_\eta$) have been obtained, except for systematically higher (by ca. 50%) reduction current densities. This difference is too high to be explained by possible underestimation of the surface area of smaller particles and, most probably, indicates particle size dependence of nitrate electroreduction.

Although the data obtained so far are not sufficient for the elucidation of the detailed mechanism of nitrate electroreduction, they allow to suggest that one-electron charge transfer to adsorbed nitrate ion is the rds on Cu-modified Pd nanoparticles. Obviously, determination of the detailed mechanism of nitrate electroreduction requires studying adsorption isotherms of possible surface intermediates, which was outside the scope of the present study.

4. Conclusions and outlook

In this work we demonstrated an approach to the *in situ* preparation of bimetallic Pd–Cu catalysts active in nitrate electroreduction by the electrochemical copper deposition on pre-formed

carbon-supported Pd nanoparticles. Electrochemical properties of Pristine Pd/C samples were studied. Hydrogen and Cu adsorption on Pd nanoparticles shows that the surface of bigger particles ($d \approx 4$ nm) contain small, but noticeable, contribution of ordered (1 1 1) and (1 0 0) facets, in agreement with HR-TEM data. This contribution decreases with the decrease of the particles size. Comparing with bulk Pd, even for bigger particles the contribution of hydrogen absorption at $E \geq 0.06$ V is small and further decreases for smaller particles. In the further studies we plan to investigate the influence of the particle size on the electrochemical properties of Pd in a wider size range.

Preparation of Pd nanoparticles modified by submonolayer amounts of Cu was performed in two steps. In the first step ca. 3 monolayers of Cu are deposited. Taking the advantage of ca. 0.15 V positive shift of monolayer versus multilayer Cu dissolution, we performed selective dissolution of the excessive amount of Cu deposited on Pd and formed bimetallic Pd–Cu surface with $\theta_{Cu} \approx 0.85$. This Cu adlayer can be further partially or completely dissolved by choosing appropriate potential thus allowing to tune Cu coverage. In a further study we will apply this approach to explore the effect of Pd–Cu surface composition on electrocatalytic properties of this bimetallic system.

Modification of metal nanoparticles by foreign metal adatoms has proven to be an efficient method to obtain well defined nanoparticulate bimetallic electrocatalysts for various processes, including CO and methanol oxidation (see e.g. [39] and refs. therein; [40]), oxygen reduction and hydrogen oxidation ([41]). In this work the modification of the surface of Pd nanoparticles with Cu adlayer resulted in pronounced increase in the nitrate electroreduction rate similar to that has previously been observed upon deposition of Cu on bulk and electrodeposited Pd. Kinetic parameters of nitrate electroreduction on Cu/Pd/C nanoparticles are similar to those observed on rough Cu-modified Pd electrodes [3,14]. In comparison to the latter the advantages of the catalysts described in this work are their well defined structure and the possibility to control and *in situ* characterize their surface composition. Armed with the procedure developed, in future studies we will focus on the structural, particle size and compositional dependencies of nitrate electroreduction on bimetallic Pd–Cu catalysts.

Acknowledgements

One of us (SP) acknowledges financial support provided by NATO Reintegration Grant (NATO RIG.981941). This work has been partially financed in the framework of the Leading Scientific School Program (Russia, Grant No. 6526.2006.3).

References

[1] T. Tacke, K.-D. Vorlop, Chem.-Ing.-Tech. 65 (1993) 1500–1502.
[2] U. Pruesse, M. Haehnlein, J. Daum, K.-D. Vorlop, Catal. Today 55 (2000) 79–90.
[3] A.C.A. de Vooys, R.A. Van Santen, J.A.R. van Veen, J. Mol. Catal. A: Chem. 154 (2000) 203–215.
[4] U. Pruesse, K.-D. Vorlop, J. Mol. Catal. A: Chem. 173 (2001) 313–328.
[5] A. Pintar, J. Batista, J. Levec, T. Kajiuchi, Appl. Catal. B: Environ. 11 (1996) 81.
[6] W. Gao, J. Chen, X. Guan, R. Jin, F. Zhang, N. Guan, Catal. Today 93–95 (2004) 333–339.
[7] W. Gao, N. Guan, J. Chen, X. Guan, R. Jin, H. Zeng, Z. Liu, F. Zhang, Appl. Catal. B: Environ. 46 (2003) 341–351.
[8] L. Lemaignen, C. Tong, V. Begon, R. Burch, D. Chadwick, Catal. Today 75 (2002) 43–48.
[9] F. Gauthard, F. Epron, J. Barbier, J. Catal. 220 (2003) 182–191.
[10] M. D'Arino, F. Pinna, G. Strukul, Appl. Catal. B: Environ. 53 (2004) 161–168.
[11] A.C.A. de Vooys, G.L. Beltramo, J.A.R. van Riet, M.T.M. Koper, Electrochim. Acta 49 (2004) 1307–1314.
[12] G.E. Dima, A.C.A. De Vooys, M.T.M. Koper, J. Electroanal. Chem. 554/555 (2003) 15–23.
[13] M.T. de Groot, M.T.M. Koper, J. Electroanal. Chem. 562 (2004) 81–94.
[14] O.A. Petrii, T.Y. Safonova, J. Electroanal. Chem. 331 (1992) 897–912.
[15] T.Y. Safonova, O.A. Petrii, J. Electroanal. Chem. 448 (1998) 211–216.
[16] E.A. Kolyadko, K. Lu Shi, B.I. Podlovchenko, Russ. J. Electrochem. 28 (1992) 312–316.
[17] Y.M. Maximov, A.S. Lapa, B.I. Podlovchenko, Russ. J. Electrochem. 25 (1989) 712–714.
[18] I.G. Casella, M. Contursi, J. Electroanal. Chem. 588 (2006) 147–154.
[19] K. Tada, T. Kawaguchi, K. Shimazu, J. Electroanal. Chem. 572 (2004) 93–99.
[20] M. Wasberg, G. Horanyi, Electrochim. Acta 40 (1995) 615–623.
[21] D. Pletcher, Z. Poorabedi, Electrochim. Acta 24 (1979) 1253–1256.
[22] P.A. Simonov, V.A. Likholobov, in: A. Wieckowski, E.R. Savinova, C.G. Vayenas (Eds.), Catalysis and Electrocatalysis at Nanoparticle Surfaces, Marcel Dekker, New York, 2003.
[23] Y.I. Ermakov, V.F. Surovkin, G.V. Plaksin, V.A. Semikolenov, V.A. Likholobov, A.L. Chuvilin, S.V. Bogdanov, React. Kinet. Catal. Lett. 33 (1987) 435.
[24] T.J. Schmidt, H.A. Gasteiger, G.D. Staeb, P.M. Urban, D.M. Kolb, R.J. Behm, J. Electrochem. Soc. 145 (1998) 2354.
[25] B.I. Podlovchenko, E.A. Kolyadko, S. Lu, J. Electroanal. Chem. 399 (1995) 21–27.
[26] A. Rose, S. Maniguet, R.J. Mathew, C. Slater, J. Yao, A.E. Russell, Phys. Chem. Chem. Phys. 5 (2003) 3220–3225.
[27] N. Hoshi, K. Kagaya, Y. Hori, J. Electroanal. Chem. 485 (2000) 55.
[28] N. Hoshi, M. Kuroda, Y. Hori, J. Electroanal. Chem. 521 (2002) 155–160.
[29] M. Hara, U. Linke, Th. Wandlowski, submitted to Electrochimica Acta, 2006.
[30] A.M. El-Aziz, L.A. Kibler, J. Electroanal. Chem. 534 (2002) 107–114.
[31] P.M. Rigano, C. Mayer, T. Chierchie, Electrochim. Acta 35 (1990) 1189–1194.
[32] P. Lenz, T. Solomun, J. Electroanal. Chem. 353 (1993) 131–145.
[33] M.Y. Rusanova, G.A. Tsirlina, O.A. Petrii, T.Y. Safonova, S.Y. Vasil'ev, Russ. J. Electrochem. 36 (2000) 457–464.
[34] A. Al-Akl, G.A. Attard, J. Phys. Chem. B 101 (1997) 4597–4606.
[35] A. Zuettel, C. Nuetzenadel, G. Schmid, D. Chartouni, L. Schlapbach, J. Alloys Compd. 293/295 (1999) 472–475.
[36] N. Tateishi, K. Yahikozawa, K. Nishimura, S. Masato, Y. Iwanaga, M. Watanabe, E. Enami, Y. Matsuda, Y. Takasu, Electrochim. Acta 36 (1991) 1235–1240.
[37] J. Solla-Gullon, A. Rodes, V. Montiel, A. Aldaz, J. Clavilier, J. Electroanal. Chem. 554/555 (2003) 273–284.
[38] S.N. Pronkin, P.A. Simonov, V.I. Zaikovskii, E.R. Savinova, in preparation (2007).
[39] F. Maillard, G.Q. Lu, A. Wieckowski, U. Stimming, J. Phys. Chem. B 109 (2005) 16230–16243.
[40] E.M. Crabb, M.K. Ravikumar, D. Thompsett, M. Hurford, A. Rose, A.E. Russell, Phys. Chem. Chem. Phys. 6 (2004) 1792–1798.
[41] K. Sasaki, Y. Mo, J.X. Wang, M. Balasubramanian, F. Uribe, J. McBreen, R.R. Adzic, Electrochim. Acta 48 (2003) 3841–3849.